Loading Behavior of p-Toluenesulfonic Acid in Biochar and its Application to Prepare 5-Hydroxymethylfurfural

Liyan Xing,[a] Rundong Liu,[a] Fanchen Jing,[a] Ming Xu,[b] and Jing He [a,*]

A carbon-based solid acid catalyst was prepared from papermaking sludge *via* calcining followed by sulfonation with p-toluenesulfonic acid. The micromorphology of several catalysts were compared *via* SEM, FT-IR, N_2 adsorption-desorption, XPS, and UV spectrum. It was found that the micromorphologies of biochar surface modified with concentrated H_2SO_4, p-toluenesulfonic acid, and sulfanilic acid were different and closely related to the binding mechanism. The biochar and p-toluenesulfonic acid exhibited π-π* stacking and hydrophobic effects. The suitable pores and gaps on the biochar surface were the key to the loading of p-toluenesulfonic acid. However, no π-π* stacking and hydrophobic effects were observed between the biochar and sulfanilic acid. The amidation grafting of sulfanilic acid to the biochar surface could lift the restriction of surface pore structure. The catalytic performance of these catalysts was evaluated *via* fructose, glucose, and cellulose degradation to 5-hydroxymethylfurfural (HMF). The HMF yield from fructose, glucose, and cellulose was 92.9%, 60.7%, and 28.6%, respectively, with the carbon-based solid acid catalyst. The carbon-based solid acid catalyst prepared from papermaking sludge and p-toluenesulfonic acid has the following advantages: a simple process, is environmentally friendly, and has good catalytic performance; as such, it has the prospect of industrialization.

INTRODUCTION

Biomass is a renewable resource that has the potential to partially or completely replace petrochemical resources; thus it may contribute to alleviating the energy crisis and the greenhouse effect (Corma *et al.* 2007). In-depth development and utilization of biomass resources is the key to solving the problems of energy exhaustion and ecological degradation. The production of high value-added chemicals and materials from biomass, *e.g.*, ethanol, 5-hydroxymethylfurfural (HMF), oligosaccharides, lignin derivatives, and cellulosic based products, has become a hot research topic (Wang *et al.* 2019; Zhang *et al.* 2020). 5-Hydroxymethylfurfural is considered to be an important platform compound that can produce various chemicals through oxidation, hydrogenation, and condensation reactions (Gandini and Belgacem 2002).

The synthesis of HMF from carbohydrates, such as fructose, glucose, and cellulose, has attracted much attention (Iris and Tsang 2017; Thoma *et al.* 2020). Fructose is the most

widely studied raw material because it is easier to prepare HMF and can achieve high HMF yield at high concentration, which is very important for industrial production. Glucose and cellulose have lower costs, and cellulose, in particular, is available from a wide range of sources. The efficient preparation of HMF from cellulose not only can greatly reduce the production cost of HMF, but it can also effectively solve various agricultural residues. Therefore, it is very important to study the applicability of catalysts to fructose, glucose, and cellulose.

Carbon-based solid acids are commonly used as heterogeneous catalysts for the preparation of HMF, which are usually prepared from various biomasses, *e.g.*, starch, glucose, straw, wood chips, and leaves (Han *et al.* 2017; Songo *et al.* 2019). The catalyst is prepared by activation pretreatment, incomplete carbonization under an inert atmosphere, sulfonation, and washing. Carbon-based solid acids have the advantages of a low cost, a wide range of raw materials, and easy recovery. The most commonly used sulfonation method is to treat biochar using concentrated sulfuric acid or fuming sulfuric acid at a high temperature (180 to 250 °C) for a long time (10 to 24 h). The -SO$_3$H is then grafted onto the surface of the biochar. However, these methods have various problems, *e.g.*, large wastewater pollution and discharge.

Researchers have attempted to incorporate sulfonic acid into biochar *via* other means to prepare carbon-based solid acids. p-Toluenesulfonic acid is organic strong acid, which can cause dehydration and carbonization of paper and wood. The sulfonic acid in p-toluenesulfonic acid has a good catalytic effect on the preparation of HMF. Shen (2016) prepared a carbon-based solid acid using waste bamboo powder as the raw material and p-toluenesulfonic acid as the sulfonating agent. The catalyst was used to catalyze fructose dehydration to prepare HMF. The HMF yield was 92.1%, which was better than the commercial ion exchange resin Amberlyst-15. Wang *et al.* (2016) prepared a new carbon-based solid acid using glucose and p-toluenesulfonic acid as the raw materials. The product was used to catalyze the dehydration of fructose to 5-hydroxymethylfurfural (HMF) and showed good catalytic performance and recycling performance. Sulfanilic acid also contains sulfonic acid, which are acidic and commonly used for modification of carbon materials (Jia *et al.* 2016; Zhao *et al.* 2018). Therefore, in the present work, sulfanilic acid and p-toluenesulfonic acid were used in an attempt to modify biochar for the preparation of HMF.

In addition, the surface structure and composition have a very important effects on the properties of a material. Many studies have shown that mesoporous materials are widely used in the field of catalysis because of their special surface aperture structure, which is conducive to modification by loading, doping, and other means, as well as having special effects on the adsorption and desorption of raw materials and products. Mesoporous materials, *e.g.*, carbon-based solid acids (Priadi *et al.* 2014), zeolites, cationic resins (Wrigstedt *et al.* 2016; Sun *et al.* 2018), and mesoporous silicon (Mérida-Morales *et al.* 2021) are widely used as solid acid catalysts or carriers for biomass dehydration. Cao *et al.* (2018) prepared a carbon-based solid acid with a high surface area using forestry wood waste and concentrated sulfuric acid. The product was used to catalyze bread waste to HMF with a yield of 30.4%. Gallo *et al.* (2016) studied the activity and stability of acid functionalized periodic mesoporic carbons (CMK-3 and CMK-5) for continuous HMF production from fructose. The catalysts had the same selectivity and turnover frequency (TOF) of propanesulfonic acid functionalized SBA-15. These carbon materials exhibit a high specific surface area, suitable pore size and stability, good catalytic activity, and cyclic stability. However, there are few reports on the etching effect of various sulfonating agents

on the biochar surface, especially the loading behavior of p-toluenesulfonic acid on the biochar surface.

In this paper, a carbon-based solid acid was prepared from papermaking sludge and modified with p-toluenesulfonic acid, concentrated sulfuric acid, or sulfanilic acid. The relationship between the micromorphology and the preparation mechanism of the catalysts was proposed. The effects of the reaction conditions on the HMF yield from fructose, glucose, and cellulose were studied. The water consumption and cycling performance of the catalyst were investigated, which provided theoretical support for industrialization.

EXPERIMENTAL

Materials

The papermaking sludge, which was generated at Nong Yuan Technology (Beijing, China) Co., Ltd, was collected from the waste liquid of chemi-mechanical pulp and air dried. The sludge was stored in a sealed bag after smashing and sieving through a 0.25 mm mesh.

The D-fructose (99%), glucose (98%), cellulose, 5-hydroxymethylfurfural (97%), tetrahydrofuran (THF), and dimethylsulfoxide (DMSO) were purchased from Shanghai Macleans Biochemical Technology Co., Ltd. (Shanghai, China).

Catalyst Preparation

Preparation of sludge biochar (SBC)

The sludge biochar (SBC) was prepared using a slight modification of the methodology reported by Cao *et al.* (2018). The samples were heated to a temperature of 300 °C at 10 °C/min and then to a temperature of 550 °C at 5 °C/min in a tube furnace under a N_2 atmosphere. The retention time at a temperature of 550 °C was 1 h.

Preparation of S-SBC, T-SBC, and A-SBC by biochar treated with concentrated sulfuric acid, p-toluenesulfonic acid, or sulfanilic acid

First, 2 g of biochar was mixed with 6 g of concentrated sulfuric acid, 6 g of p-toluenesulfonic acid, or 6 g of sulfanilic acid in a 25 mL hydrothermal kettle. The three samples were heated at a temperature of 200 °C for 6 h in a muffle furnace and then transferred to crucibles for aging at a temperature of 150 °C for 4 h.

After the reaction, the mixture was washed and filtered with a large amount of deionized water (at a temperature of 80 °C) until the filtrate was neutral and the water consumption was recorded. The samples were dried at a temperature of 105 °C for 4 h and stored in sealed bags. The three samples were labeled as S-SBC, T-SBC, and A-SBC, respectively.

Preparation of A-G-SBC by biochar grafted with sulfanilic acid

First, 6 g of biochar was added to 60 mL of a 20% hydrogen peroxide solution and stirred at room temperature for 24 h. The remaining solid was filtered and fully washed with deionized water. The oxidized biochar was obtained after being dried in an oven at a temperature of 105 °C for 4 h. Then, 2 g of oxidized biochar, 4 g of sulfanilic acid, and 20 mL of deionized water were mixed in a 100 mL three-mouth flask.

The mixture was thoroughly stirred at a temperature of 100 °C for 30 min, dried and cooled to room temperature. Next, 40 mL of hydrochloric acid solution (9.6 mol/L)

was added into the remaining solid and reacted at a temperature of 100 °C for 45 min. The mixture was strained while it was hot, and the biochar (A-G-SBC) grafted *via* sulfanilic acid was obtained after being dried at a temperature of 105 °C for 4 h (Jia *et al.* 2016).

Catalyst Characterization

Fourier-transform infrared spectroscopy (FTIR) (Nicolet iS 5, Thermo Fisher Scientific, Waltham, MA) was performed using the KBr method. The sample was mixed with a KBr medium, and the experiments were carried out over a scanning range of 400 to 4000 cm^{-1}.

The microstructure and morphology of the biochar were examined *via* cold field emission scanning electron microscopy (FE-SEM JSM -6700F, Jeol, Tokyo, Japan).

Powder X-ray diffraction (XRD) (X'Pert PRO MPD, Panalytical, Holland, Netherlands) was performed at a 0.02° step and 5° to 90° 2θ range in continuous scanning mode; the radiation source was Cu target and calculated using the Jade software (version 6, MDI, Livermore, CA).

The N_2 adsorption-desorption experiment was recorded at a temperature of -196 °C using an ASAP 2020 Plus 1.03 specific surface and pore size analyzer. The biochar samples were degassed at a temperature of 150 °C for 8 h. The specific surface area, pore volume, and mean pore diameter were obtained using the Brunauer-Emmett-Teller (BET) method and the Barrett-Joyner-Halenda (BJH) method.

The surface chemical composition and the chemical state of the functional groups on the biochar samples were determined *via* X-ray photon spectroscopy (XPS) (EscaLab Xi+, Thermo Fisher Scientific, Waltham, MA).

The content of the metal ions was determined via inductively coupled plasma optical emission spectrometry (ICP-OES) (iCAP Q, Thermo Fisher Scientific, Waltham, MA). The samples were digested in 5 mL of HNO_3 and 3 mL of hydrofluoric acid at a temperature of 180 °C.

The total acid sites and the -SO_3H content on the biochar surfaces were tested using an acid-base titration experiment (Boehm 1994; Wang *et al.* 2011). The total number of acid sites was measured using the following method. Briefly, 250 mg of catalyst was dispersed in 30 mL of a sodium hydroxide solution (0.05 mol/L) under ultrasound for 60 min. The supernatant solution obtained *via* filtration was titrated with a hydrochloric acid standard solution (0.05 mol/L) using phenolphthalein as an indicator. The -SO_3H content was measured using the following method. A 250 mg sample of the catalyst was dispersed in 30 mL of a standard sodium chloride solution (0.05 mol/L) under ultrasound for 60 min to replace the H^+ ions in the catalyst. Phenolphthalein was then used as an indicator, and the supernatant solution obtained *via* filtration was titrated with a sodium hydroxide aqueous solution (0.05 mol/L).

To analyze the UV spectrum, 0.5, 1, and 2 g biochar were mixed with 2.33 g of concentrated sulfuric acid, 2.33 g of p-toluenesulfonic acid, and 2.33 g of sulfanilic acid, respectively, in a hydrothermal reactor and calcined at a temperature of 200 °C for 6 h in a muffle furnace. Then the three samples was transferred to a crucible at a temperature of 105 °C aged for 4 h. Then, 50 mL of deionized water was added and subjected to ultrasound for 30 min. The filtrate with fine biochar particles was obtained *via* filtering. A small amount of filtrate was taken for full UV spectrum scanning and labeled as A, B, and C, respectively.

Effects of the reaction temperature and time on the 5-hydroxymethylfurfural (HMF) yield

First, 100 mg of fructose, 100 mg of the catalyst, and 5 mL of a H$_2$O/DMSO (V/V, 0.5 to 4.5) solution were mixed in a thick wall glass reactor, followed by being heated at the set temperature for a set time. The reactor was cooled in an ice bath after the reaction.

Effect of the modifier dosage on the 5-hydroxymethylfurfural (HMF) yield

First, 2 g of biochar was mixed with different amounts of p-toluenesulfonic acid (1.5, 3, 6, and 1 2g), concentrated sulfuric acid (6, 12, and 24 g), or sulfanilic acid (6, 12, and 24 g) in a hydrothermal kettle and calcined at a temperature of 200 °C for 6 h. Then the samples were transferred to crucibles for aging at a temperature of 150 °C for 4 h. The samples were washed with deionized water (at a temperature of 80 °C) until neutral and then dried at a temperature of 105 °C for 4 h.

The biochar catalysts were labeled as T-SBC1, T-SBC2, T-SBC, T-SBC3, S-SBC, S-SBC1, S-SBC2, A-SBC, A-SBC1, and A-SBC2 in sequence. The HMF was prepared *via* the dehydration of fructose under optimal reaction conditions, and the catalytic activity of each catalyst was determined.

Effects of the calcination temperature and time on the 5-hydroxymethylfurfural (HMF) yield

First, 2 g of biochar was mixed with 6 g of p-toluenesulfonic acid and 24 g of sulfanilic acid in a hydrothermal kettle and calcined at a set temperature for the set time. The samples were washed with deionized water (at a temperature of 80 °C) until neutral and then dried at a temperature of 105 °C for 4 h. The HMF was prepared *via* the dehydration of fructose under optimal reaction conditions, and the catalytic activity of each catalyst was determined.

Catalytic performance for glucose and cellulose

First, 125 mg of glucose or cellulose, 100 mg of catalyst, 10 mL of H$_2$O/THF (1 to 4 ratio, v/v), and 0.875 g of NaCl were mixed in a high-pressure reactor, and then heated at a temperature of 160 °C for 3 h. The reactor was cooled in an ice bath after the reaction.

Products Analysis

The reaction products were filtered through a 0.22 µm organic needle filter, which was composed of polypropylene shell and Teflon filter membrane (Haiyan New Oriental Plasticizing Technology Co., LTD., Jiaxing, Zhejiang Province, China). The filtrate was diluted to a suitable concentration with deionized water. Quantitative analysis of the HMF was performed *via* high-performance liquid chromatography (HPLC) with a UV detector and a VYDAC 214TP54 column (C18, 5 μm, 250 mm × 4.6 mm). A water and methanol solution (80 to 20 ratio, v/v) was used as the mobile phase at a flow rate of 0.6 mL/min at a column temperature of 30 °C. The standard curve line of HMF was prepared using pure HMF as the standard.

The yield of HMF was calculated according to Eq. 1,

$$\text{HMF Yield (\%)} = \frac{\text{moles of HMF}}{\text{moles of starting C6 carbohydrate}} \times 100 \qquad (1)$$

where the moles of the starting C6 carbohydrate were fructose, glucose, or cellulose.

RESULTS AND DISCUSSION

Catalyst Characterization

SEM images

Noticeable differences in the micromorphology were observed among these solid acid catalysts (Fig. 1). The SEM image of SBC clearly showed an irregular morphology with stratified channels, pores, and ridged surfaces (Cao *et al.* 2018). The structure was similar to the straw fiber structure but different from the planar structure of biochar derived from sugar (Bai *et al.* 2015; Zhao *et al.* 2016).
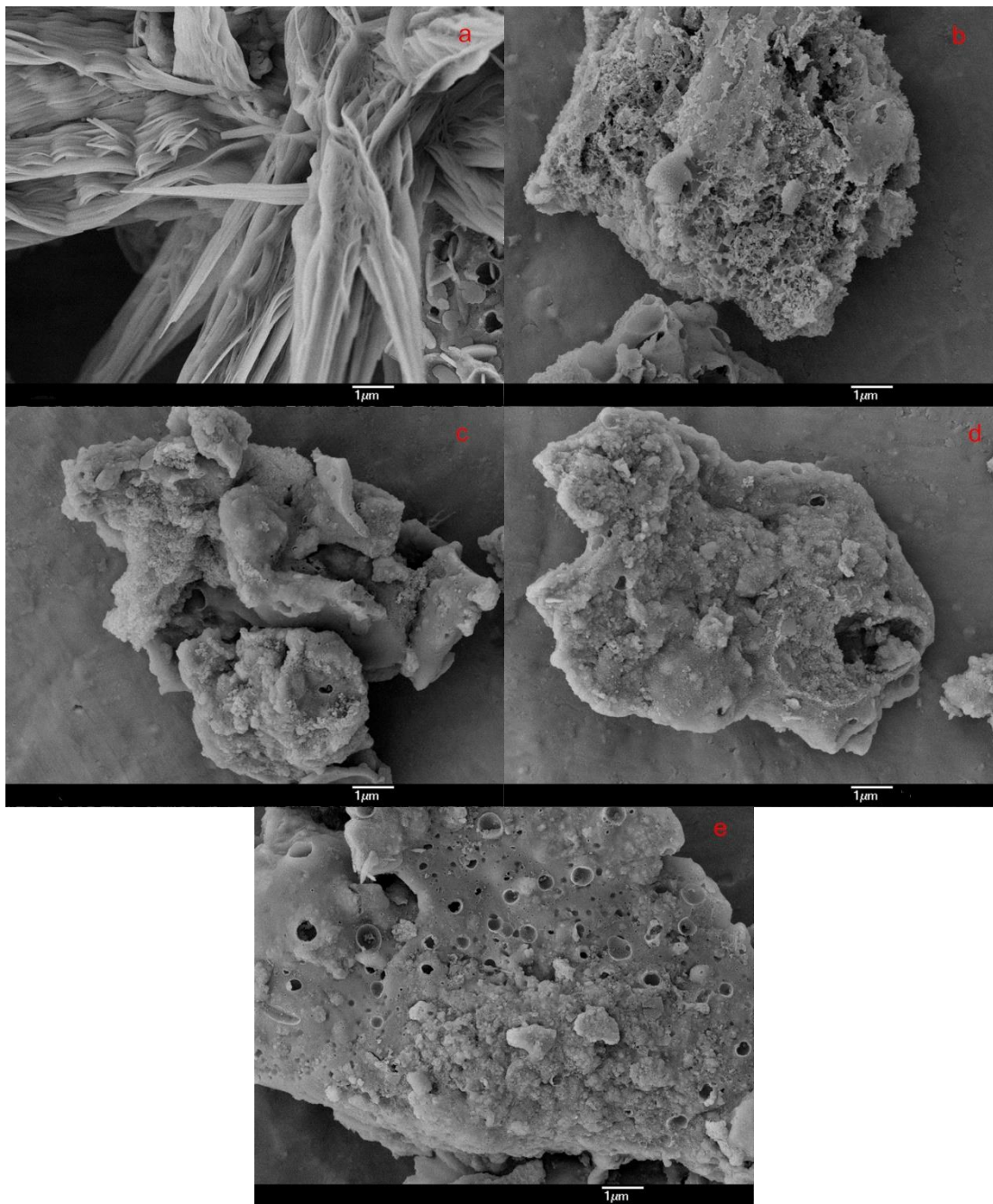

Fig. 1. SEM images of SBC (a); T-SBC (b); S-SBC (c); A-SBC (d); and A-G-SBC (e)

The ridge structure of T-SBC was destroyed in the treatment process, and a large number of homogeneous pore structures were formed. As p-toluenesulfonic acid is a strong acid, it had a considerable corrosive effect on the surface of the biochar. The large pores of T-SBC were formed because of the large molecular structure of p-toluenesulfonic acid. The unique structure showed a larger surface area and surface active center, which can considerably improve the catalytic performance. The surface of S-SBC presented a loose gap structure with many particle structures. Probably as the molecular structure of sulfuric acid was smaller than p-toluenesulfonic acid, it can form many small particles with similar diameters on the surface of the biochar. In addition, the distribution of particles was uniform, regular, and orderly. The surface structure of A-SBC was similar to the surface structure of S-SBC. There were small particles on the surface, but no pores and gaps were formed, which may be due to the weak corrosive effect of sulfanilic acid on biochar. The surface of A-G-SBC simultaneously had small particles and pores of different sizes, which was the result of the interaction of the hydrochloric acid and sulfanilic acid.

FTIR spectra of the catalysts

In order to study the introduction of $-SO_3H$ in various catalysts, the types and structures of the functional groups of biochar were studied *via* the FTIR spectra (as shown in Fig. 2). The bands at 1600 cm^{-1} were assigned to the stretching vibration of the polycyclic aromatic hydrocarbon skeleton (Chen and Fang 2011; Xu *et al.* 2015). The band appearing at 799 cm^{-1} for the S-SBC, T-SBC, A-SBC, and A-G-SBC samples was assigned to the absorption peak of the substituent of the benzene ring, which indicated that the $-SO_3H$ groups were attached to the surface of the biochar or grafted onto the benzene ring of the biochar.
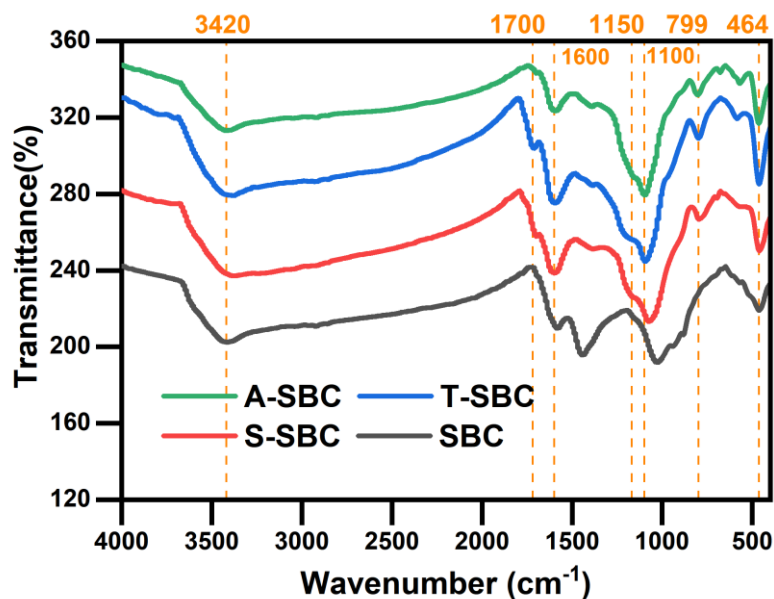

Fig. 2. The FTIR spectra of SBC, T-SBC, S-SBC, A-SBC, and A-G-SBC

The bands at 1100 cm^{-1} and 464 cm^{-1} of the T-SBC, S-SBC, A-SBC, and A-G-SBC samples represented the stretching vibration and rocking vibration of Si-O-Si from ash, which were sharper than the bands of SBC (Kim *et al.* 2010). The sharper peak of Si-O-Si in the S-SBC, T-SBC, A-SBC, and A-G-SBC samples was due to the dissolving of

inorganic salt during sulfonation. The band at 1700 cm^{-1} was assigned to the S=O stretching vibration (Toda *et al.* 2005; Songo *et al.* 2019). There was no peak for SBC at 1700 cm^{-1} and the peak intensity of the remaining catalysts at approximately 1700 cm^{-1} were ranked as follows: T-SBC was greater than S-SBC, which was approximately equal to A-G-SBC, which was greater than A-SBC. This result indicated that the -SO$_3$H group was successfully introduced to the surface of the T-SBC, S-SBC, and A-G-SBC samples, while that of A-SBC may be insufficient. The new band at 1150 cm^{-1} for the T-SBC, S-SBC, A-SBC, and A-G-SBC samples was assigned to the O=S=O anti-symmetric stretching vibration, which showed the same trend of peak at 1700 cm^{-1} (Hara *et al.* 2004). The peaks at 1150 cm^{-1} and 1700 cm^{-1} of T-SBC, S-SBC, A-SBC, and A-G-SBC also represent the successful introduction of -SO$_3$H.

Textural properties of the catalysts

The specific surface area and total pore volume of a catalyst are important parameters of heterogeneous catalysis. The textural properties of various catalysts are shown in Table 1. The surface area of SBC was very small, only 0.2 m^2·g^{-1}, while the surface area and total pore volume of T-SBC, S-SBC, A-SBC, and A-G-SBC were considerably larger, which indicated that the new pores or gaps were generated after modification. The surface area of T-SBC, S-SBC, and A-G-SBC increased to more than 80 m^2·g^{-1}, while the surface area of A-SBC was only 46.1 m^2·g^{-1}. The micropores of S-SBC, A-G-SBC, and A-SBC accounted for 44.4%, 32.0%, and 59.2% of the pore volume, respectively, while they only accounted for 2.1% for T-SBC. According to the adsorption and desorption isotherms in Fig. 3 (small), all catalysts displayed a Type IV isotherm, characteristic of mesoporous materials (Thommes *et al.* 2015).
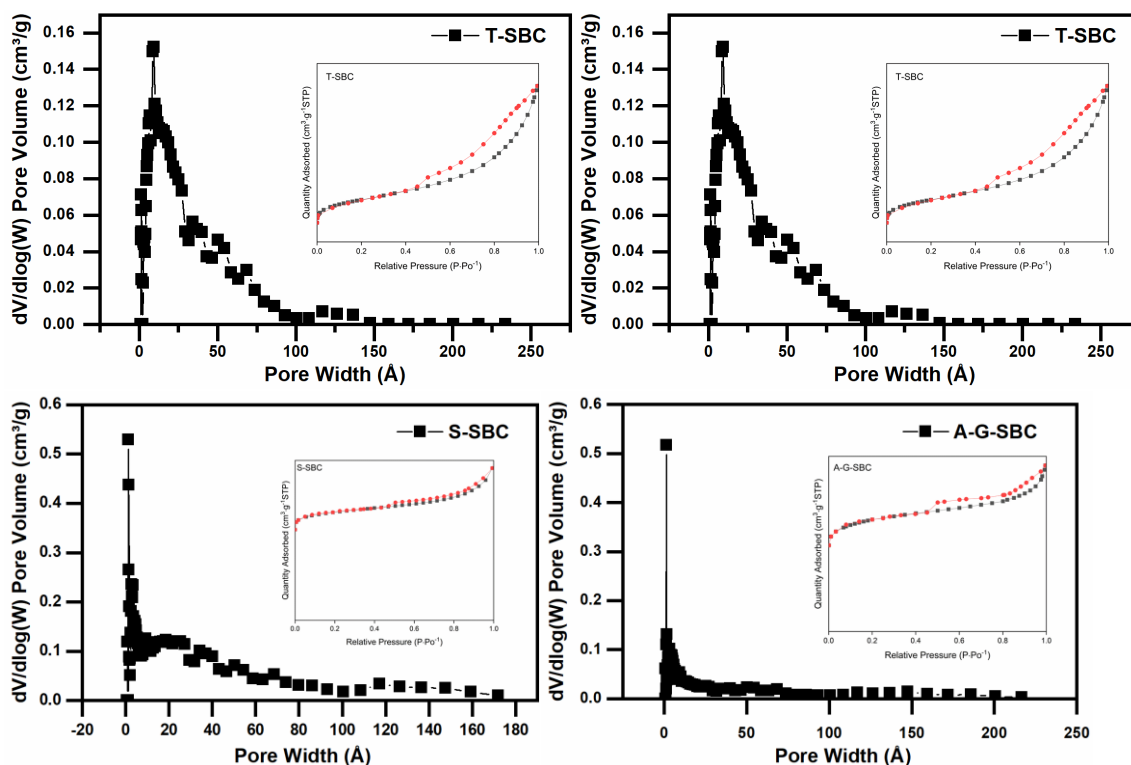

Fig. 3. Pore size distribution (large) and N$_2$ adsorption-desorption isotherms (small) of T-SBC, S-SBC, A-SBC, and A-G-SBC

Most of the mesoporous aperture of S-SBC, A-G-SBC, and A-SBC was in the range of 2 to 10 nm, while that of T-SBC was 10 to 50 nm (Fig. 3-large). Both S-SBC and A-SBC were prepared by calcination and had a similar aperture structure, while -SO$_3$H can be successfully introduced to S-SBC but was insufficient in A-SBC, according to the FTIR results. Therefore, it was speculated that sulfuric acid molecules could be adsorbed into micropores and small mesoporous (5 to 10 nm) of biochar and combined well with it. However, the amount of sulfanilic acid may be insufficiently adsorbed into the micropores and small mesopores (5 to 10 nm), resulting in insufficient introduction of -SO$_3$H into A-SBC.

The preparation method of T-SBC was the same as that of S-SBC and A-SBC but had a larger mean pore size. The peak intensity of T-SBC was much larger than that of A-SBC according to the FTIR. Suitable pore sizes may be favorable for the loading of p-toluenesulfonic acid and was bound closely with biochar *via* some kind of binding force.

A-G-SBC was prepared by amidation but had a similar aperture structure with S-SBC and A-SBC. The peak intensity of A-G-SBC was approximately equal to S-SBC and much larger than A-SBC. The -SO$_3$H grafted onto the surface of biochar by amidation may remove the limitation of surface pore size and successfully introduce -SO$_3$H to A-G-SBC.

Table 1. Textural Properties of the T-SBC, SBC, S-SBC, A-SBC, and A-G-SBC Samples

Samples	S_{BET} (m^2·g^{-1})	S_{micro} (m^2·g^{-1})	Ratio of Micropores (%)	V_t (cm^3/g)[a]	D^c (nm)[b]
SBC	0.2	2.8	-	0.0015	-
T-SBC	83.6	1.8	2.1	0.1737	8.3
S-SBC	89.8	39.9	44.4	0.1022	4.6
A-SBC	46.1	27.3	59.2	0.0569	3.4
A-G-SBC	169.5	54.3	32.0	0.023	5.4
Note: [a] Total pore volume; and [b] Average pore diameter					

The analysis of the UV spectrum

Biochar modified with concentrated sulfuric acid and grafted with sulfanilic acid has been extensively studied, and the reaction mechanism is relatively clear. The mechanism of S-SBC is as follows: the residual H atoms in the aromatic ring are replaced by -SO$_3$H. The mechanism of A-G-SBC is as follows: the amino group in the sulfanilic acid was aminated with carboxyl on the surface of biochar, and then grafted onto the surface of the biochar. However, the mechanism of biochar treated with p-toluenesulfonic acid is still unclear. In order to study the interaction between p-toluenesulfonic acid and biochar, the samples were tested *via* UV spectrum.

The electron-supplying capacity of biochar is derived from the phenolic hydroxyl structure of biochar, especially biochar prepared *via* cryogenic pyrolysis, which has a higher phenolic hydroxyl content. The -SO$_3$H in p-toluenesulfonic acid and sulfanilic acid is a strong electron-withdrawing group, which causes the π electron from the benzene ring to transfer to -SO$_3$H. Typically, π-π* stacking occurs between electron-rich and electron-poor aromatic compounds. Therefore, π-π* stacking takes place between the electron-rich biochar aromatic ring and the electron-poor benzene ring of p-toluenesulfonic acid or sulfanilic acid. Biochar contains a large number of aromatic ring structures that may increase the force of π-π* stacking. The π-π* stacking structures are shown in Fig. 4 (Peng 2013; Pang and Wang 2014).
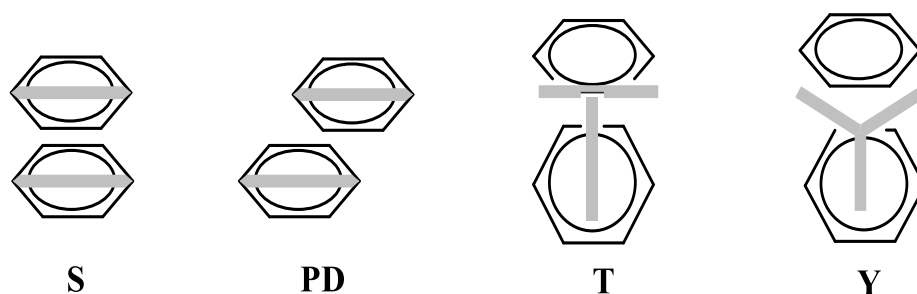
Fig. 4. The π-π* stacking structure: S: Sandwich stack; PD: parallel stacking; T: T-type stacking; and Y: Y type stacking

Figure 5 shows the UV spectra of the suspensions of biochar and p-toluenesulfonic acid or sulfanilic acid. The peaks near 260 and 220 nm are the K-band and R-band generated by the π-π* electron transition of p-toluenesulfonic acid and sulfanilic acid, respectively. The maximum absorption wavelength of the K-band near 220 nm of p-toluenesulfonic acid was blue shifted as the addition of biochar increased (as shown in Fig 5a). The peak intensity at approximately 220 nm and 260 nm decreased perhaps because the biochar and p-toluenesulfonic acid experienced the force of π-π* stacking. The steric hindrances of the p-toluenesulfonic acid molecules increased due to the aromatic ring structure of the biochar particles, and the shape and distribution of the π electron cloud changed, which decreased the electron mobility and conjugation effect. Thus, the peak intensity decreased. However, no obvious blue shift and reduced peak intensity were observed in the UV spectra of the suspension of biochar and sulfanilic acid (as shown in Fig. 5b); therefore, no π-π* stacking occurred between the biochar and sulfanilic acid. It was speculated that most of it was present in the form of an inner salt and does not form suitable sites for the loading of sulfanilic acid, resulting in sulfanilic acid not binding to biochar in large quantities.
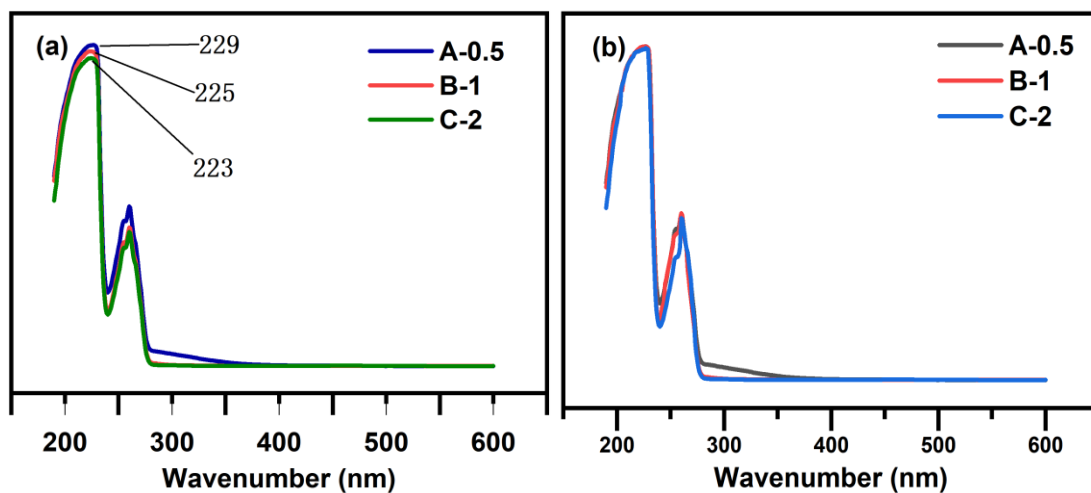

Fig. 5. The UV-Vis spectrum of p-toluenesulfonic acid and biochar filtrate: A-0.5: 0.5 g of biochar and 2.33 g of benzenesulfonic acid; B-1: 1 g of biochar and 2.33 g of benzenesulfonic acid; and C-2: 2 g of biochar and 2.33 g of benzenesulfonic acid

Table 2. Surface Composition (wt%) and Acidity of the Biochar

		C (%)	N (%)	O (%)	S (%)	Si (%)	Total Acidity (mmol/g)	-SO₃H Acidity (mmol/g)
1	SBC	57.48	1.93	37.51	0.29	2.79	-	-
2	T-SBC	63.19	1.8	25.74	1.65	7.62	3.11	0.92
3	S-SBC	61.02	2.57	28.44	0.5	7.47	1.56	0.21
4	A-SBC	60.64	4.15	28.57	0.44	6.2	0.34	0.11
5	A-G-SBC	64.01	3.3	24.75	0.92	7.02	3.32	0.8
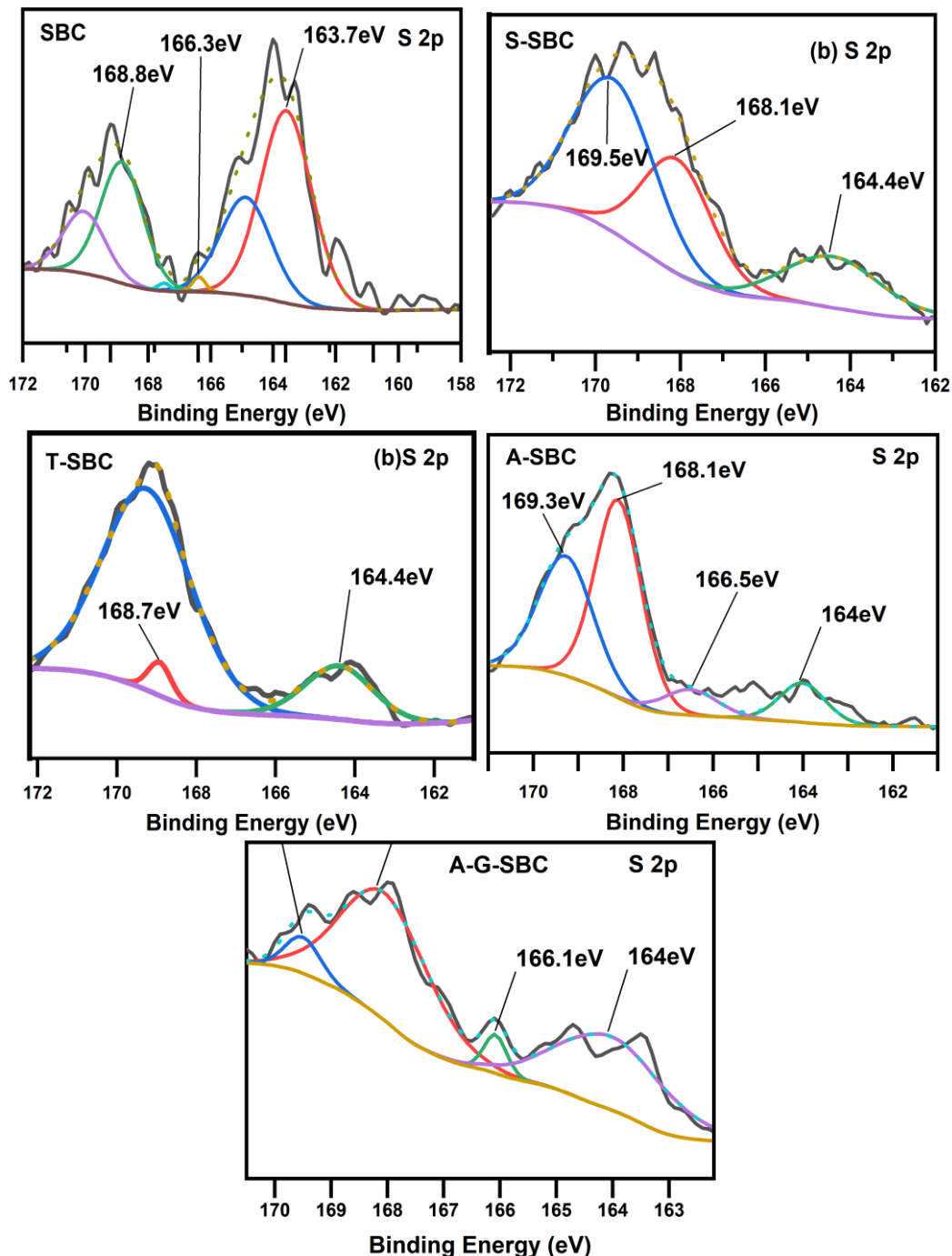
Fig. 6. The chemical state of sulfur in the SBC, S-SBC, T-SBC, A-SBC, and A-G-SBC samples

Surface composition and chemistry of SBC, S-SBC, T-SBC, A-SBC, and A-G-SBC

In order to further explore the introduction mechanism of -SO$_3$H, the surface composition and chemical state of sulfur in the biochar were analyzed *via* high-resolution XPS. The content of sulfur in SBC was 0.29%, while it increased in T-SBC, S-SBC, A-SBC, and A-G-SBC, confirming the incorporation of sulfur. In addition, T-SBC was found to have the highest sulfur content, which was greater A-G-SBC, which was greater S-SBC and A-SBC. As shown in Fig. 5, in the detailed S2p track scan of SBC, the strong peak of 163.7 eV indicated that the sulfur in SBC primarily was present in the form of -SH. The peak at 164 eV for S-SBC, T-SBC, A-SBC, and A-G-SBC was weakened, while the peak at 168.7 eV and 169.2 eV increased, which indicated that the sulfur elements in S-SBC, T-SBC, A-SBC, and A-G-SBC primarily were present in the form of -SO$_3$H. The introduction of sulfur in the sulfonation process was further confirmed.

The acid-base titration experiments of the S-SBC, T-SBC, A-SBC, and A-G-SBC samples

Acid-base titration experiments can further illustrate the introduction of -SO$_3$H. Because the SBC was alkaline, no acid base titration was performed. According to the acid-base titration results, the total acidity of T-SBC was 3.11 mmol/g, which was slightly lower than the total acidity of A-G-SBC, and much higher than the total acidity of S-SBC and A-SBC (as shown in Table 2). The total acidity of A-G-SBC was greater than the total acidity of T-SBC because A-G-SBC contained more oxygen-containing functional groups due to H$_2$O$_2$ oxidization. In addition, the hydrochloric acid residue in A-G-SBC may be another reason for the increase in the total acidity. However, the acidity of -SO$_3$H in T-SBC was 0.92 mmol/g, which was higher than the acidity in A-G-SBC (0.8 mmol/g). This indicated that the -SO$_3$H introduced *via* calcination of p-toluenesulfonic acid and biochar was more than the amount introduced *via* grafting. The total acidity and -SO$_3$H acidity of A-SBC were the lowest, which may be due to the weak acidity and high melting point of sulfanilic acid. Sulfanilic acid reacted with biochar in the solid form because the calcination temperature did not reach the melting point of sulfanilic acid. T-SBC, S-SBC and A-SBC had similar preparation methods. A-SBC had a similar surface pore structure with S-SBC but lower amount of -SO$_3$H, and T-SBC had larger mean pore size but higher amount of -SO$_3$H than A-SBC. Therefore, it was speculated that the introduction of -SO$_3$H may be related to the surface pore structure.

Catalytic Performance

Effects of the reaction temperature and time on the 5-hydroxymethylfurfural (HMF) yield

As shown in Fig. 7a, T-SBC had the best HMF yield of 92.9% at a temperature of 140 °C for 80 min. The S-SBC sample had the second-best yield, with a highest HMF yield of 56.3% (Fig. 7b). However, A-SBC had almost no catalytic activity (Fig. 7c). The results were consistent with the characterization of catalysts. The high catalytic activity of T-SBC was related to its micromorphology. On the one hand, it may be that the larger mesopore (10 to 50 nm) content was conducive to the loading of p-toluenesulfonic acid. On the other hand, macroporous and mesoporous pores are favorable for the adsorption and desorption of reactants and products. There were mainly micropores on the surface of A-SBC, which was not conducive for sulfanilic acid to enter the micropores and combine with the surface. When sulfanilic acid was grafted onto the surface of biochar *via* amidation grafting, it was no longer limited by the surface pores, and the catalytic activity was greatly increased (Table 3). The best HMF yield of A-G-SBC was 95.2% at a temperature of 130 °C for 40 min.
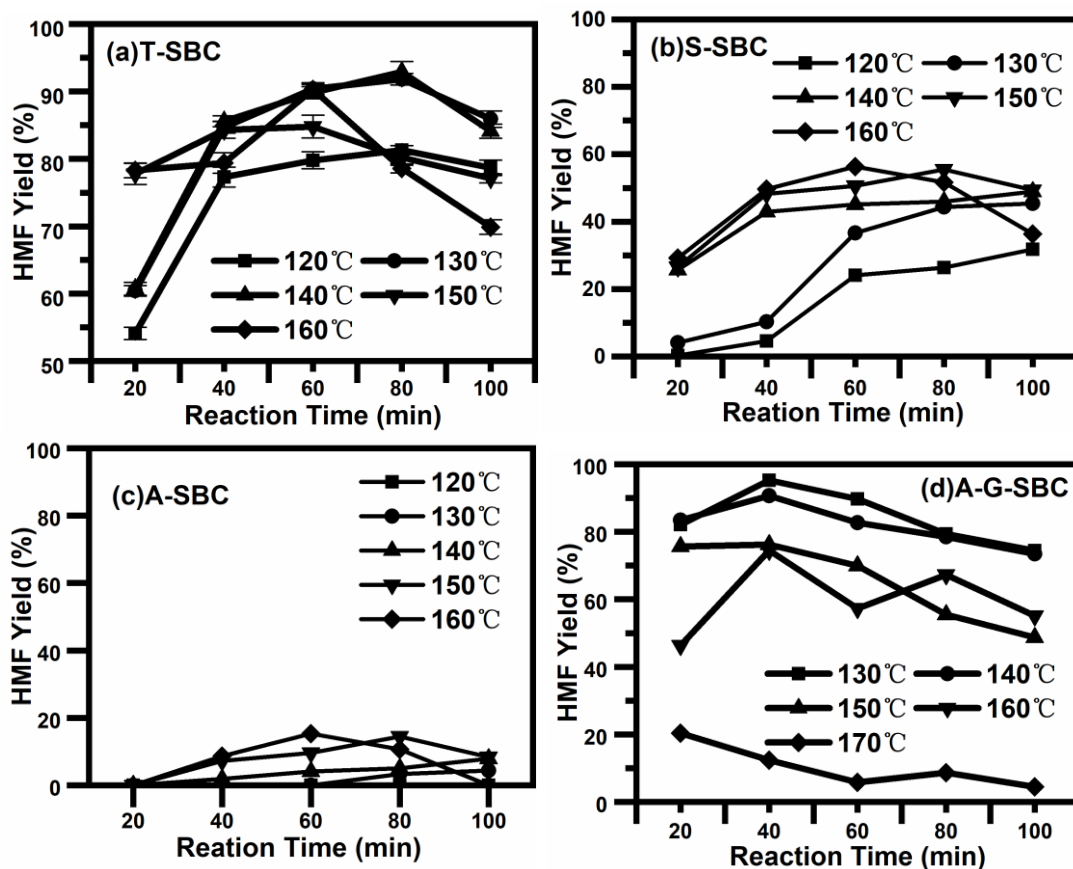
Fig. 7. Change in the HMF yield with the reaction temperature and time with various catalysts, *i.e.*, fructose (100mg), catalyst (100 mg), and H_2O to DMSO (0.5 to 4.5, v/v).

Table 3. Surface Morphology and 5-hydroxymethylfurfural (HMF) Yield of Various Catalysts

Characteristics		Catalyst				
		SBC	T-SBC	S-SBC	A-SBC	A-G-SBC
SEM		Ridged surfaces	Larger mesoporous (10~50nm)	Particles, loose gaps	Particles, tightness	Particles, gaps (different sizes)
FTIR	1700 cm^{-1} (S=O)	no	large	middle	small	middle
	1150 cm^{-1} (O=S=O)	no	large	middle	small	middle
micropores[a] (%)		-	2.1	44.4	59.2	32
π-π* Stacking[b]		-	yes	-	no	-
S[c] (%)		0.29	1.65	0.5	0.44	0.92
Total Acidity (mmol/g)		-	3.11	1.56	0.34	3.32
-SO₃H Acidity (mmol/g)		-	0.92	0.21	0.11	0.8
HMF yield[d] (%)		-	92.9	56.3	19.6	95.2
Note: [a]: The ratio of the micropores; [b]: Determined *via* UV spectrum; [c]: Determined *via* XPS; and [d]: Under optimal reaction conditions						

The significant characteristics of several catalysts are compared in Table 3. The T-SBC prepared by simple calcination method had the fewest micropores (2.1%), the largest infrared characteristic peak of -SO$_3$H, the highest relative sulfur content (1.65%), and the highest HMF yield (92.9%).

The SBC was unable to catalyze fructose dehydration to prepare HMF because it was alkaline. The p-toluenesulfonic acid reacted with the residual alkalis in the biochar and etched the surface of the biochar. A small amount of p-toluenesulfonic acid was rapidly consumed by the alkaline substances, and the catalytic activity of T-SBC1 was poor (Table 4). With the increase in the p-toluenesulfonic acid dosage, the pore structure of the biochar surface became richer, and the HMF yield also increased (Table 4). The HMF yield remained unchanged as the amount of p-toluenesulfonic acid was excessive. When the pore structure on the surface of the biochar is rich enough, the surface area and pore structure of the biochar cannot further improve by increasing the amount of p-toluenesulfonic acid; therefore, the HMF yield could not continue to increase (Table 4). The highest HMF yield with T-SBC was 92.9%, and the water consumption was 750 mL (Table 4). With the increase in the sulfuric acid dosage, the HMF yield rapidly increased, but the water consumption also greatly increased (Table 4). Increasing the amount of sulfanilic acid hardly improved the HMF yield, which was only 20.5% with A-SBC2 (as shown in Table 4). The preparation of A-G-SBC needed to go through two steps, *i.e.*, oxidation and amidation grafting. The A-G-SBC sample removed the restrictions of the pore structure on the surface and had high catalytic activity in terms of HMF preparation. However, the water consumption of A-G-SBC was greatly increased (2500 mL), which was much higher than the water consumption of the p-toluenesulfonate methods (750 mL).

Table 4. Catalyst Activity and Water Consumption

	Sample	Acid Types	Dosage of Acid (g)	V_n (mL)	HMF Yield (%)
1	SBC[a]	-	-	-	-
2	T-SBC1[b]	p-toluenesulfonic acid	1.5	100	15
3	T-SBC2[b]	p-toluenesulfonic acid	3	300	64.8
4	T-SBC[b]	p-toluenesulfonic acid	6	750	92.9
5	T-SBC3[b]	p-toluenesulfonic acid	12	1300	92.5
6	S-SBC[a]	concentrated sulfuric acid	6	900	56.3
7	S-SBC1[a]	concentrated sulfuric acid	12	1500	73.7
8	S-SBC2[a]	concentrated sulfuric acid	24	2300	90.3
9	A-SBC[a]	sulfanilic acid	6	300	10.6
10	A-SBC1[a]	sulfanilic acid	12	700	15.3
11	A-SBC2[a]	sulfanilic acid	24	1600	20.5
12	A-G-SBC[c]	sulfanilic acid	4	2500	95.2

Note: - Not checked out or added; V_n: Water consumption of catalyst when washed to neutral; [a]: catalyst (100 mg), H$_2$O/DMSO (0.5 to 4.5 v/v), 160°C, 60 min; [b]: catalyst (100 mg), H$_2$O/DMSO (0.5 to 4.5 v/v), 140°C, 80 min; and [c]: catalyst (100 mg), H$_2$O/DMSO (0.5 to 4.5 v/v), 130 °C, 40 min

Effects of calcination temperature and time on the 5-hydroxymethylfurfural (HMF) yield

The calcination time of the biochar and p-toluenesulfonic acid had little effect on HMF yield (Table 5). However, the calcination temperature had considerable influence on the HMF yield. Since the melting point of p-toluenesulfonic acid is 106 °C, the p-toluenesulfonic acid was in solid form at 100 °C, which had a limited effect on the etching of the biochar surface (Table 5). P-toluenesulfonic acid exists in the form of a liquid and

gas when the calcination temperature exceeds the boiling point, and a large number of pores and gaps were formed on the surface of the biochar. P-toluenesulfonic acid could enter the pores and bind closely to the surface of the biochar. When the calcination temperature was 150, 200, or 250 °C, the HMF yield was much higher than the HMF yield at 100 °C (Table 5).

Table 5. Effects of Different Calcination Temperatures and Times of the Catalysts on the 5-hydroxymethylfurfural (HMF) Yield

	Acid Types	Calcination Temperature (°C)	Calcination Time (h)	HMF Yield (%)
1	p-toluenesulfonic acid[a]	200	2	88.2
2	p-toluenesulfonic acid[a]	200	4	89.4
3	p-toluenesulfonic acid[a]	200	6	92.9
4	p-toluenesulfonic acid[a]	200	8	90.8
5	p-toluenesulfonic acid[a]	100	2	30.4
6	p-toluenesulfonic acid[a]	150	2	87.9
7	p-toluenesulfonic acid[a]	250	2	88.5
8	sulfanilic acid[b]	200	6	20.5
9	sulfanilic acid[b]	200	10	19.6
10	sulfanilic acid[b]	250	6	21.3
11	sulfanilic acid[b]	350	6	30.8

Note: [a]: 2 g of biochar was sulfonated by 6 g of p-toluenesulfonic acid, catalyst (100 mg), H_2O/DMSO (0.5 to 4.5 ratio v/v), 160 °C, 60 min; and [b]: 2 g of biochar was sulfonated by 24 g of sulfanilic acid, catalyst (100 mg), H_2O/DMSO (0.5 to 4.5 ratio v/v), 140 °C, 80 min

Prolonging the calcination time had no effect on the HMF yield using sulfanilic acid as the sulfonating agent (Table 5). The HMF yield slightly improved when the calcination temperature was increased to 350 °C, which exceeded the boiling point of sulfanilic acid. The HMF yield (30.8%) was much lower than the HMF yield of p-toluenesulfonic acid. The sulfanilic acid, which mostly existed in the form of inner salt, decreased the etching effect of sulfanilic acid on biochar.

Catalytic performance for glucose and cellulose

The catalytic performance of these catalysts on glucose and cellulose was tested and shown in Fig. 8. Studies show that HMF prepared with glucose and cellulose has a good yield in the THF/H_2O-NaCl solvent system (He *et al.* 2018; Cao *et al.* 2019). In this experiment, the catalytic performance of these catalysts in terms of glucose and cellulose was tested using the THF/H_2O-NaCl solvent system. The T-SBC, S-SBC2, and A-G-SBC samples all had good catalytic activity in terms of HMF preparation from glucose, with HMF yields of 60.7%, 43.7%, and 54.1%, respectively. Numerous studies have shown that the presence of a Lewis acid is the key to the isomerization of glucose into fructose, thus improving the yield of HMF. It is speculated that a large number of metal ions were concentrated in the papermaking sludge, which can act as the Lewis acid sites for the catalysts (Zhang *et al.* 2017).

Mérida-Morales *et al.* (2021) reported the morphology of several mesoporous silicas was key to the dehydration of glucose to HMF. The presence of too many micropores was not conducive to the diffusion of the reactants and products, which easily caused blockages in the pore structure and deactivated the catalyst. The HMF yield from fructose using T-SBC, S-SBC, and A-G-SBC was similar, but it was considerably different from

glucose and cellulose. The HMF yield from glucose using T-SBC was much higher than the HMF yield using S-SBC2. Since less humus was produced during fructose conversion, the pore structure and active sites of S-SBC2 were not blocked. Additional humus would be generated in the conversion process of glucose and cellulose, resulting in the blockage of the pore structure and the active sites of the catalyst. However, the pore structure of the T-SBC sample was not blocked by humus, which was primarily mesoporous and macroporous. Although the -SO$_3$H in A-G-SBC was not restricted by the surface pore structure, the Lewis acid sites in the micropores would be inactivated due to the blocking by the humus. Therefore, the catalytic activity of A-G-SBC was lower than the catalytic activity of T-SBC, but better than the catalytic activity of S-SBC.
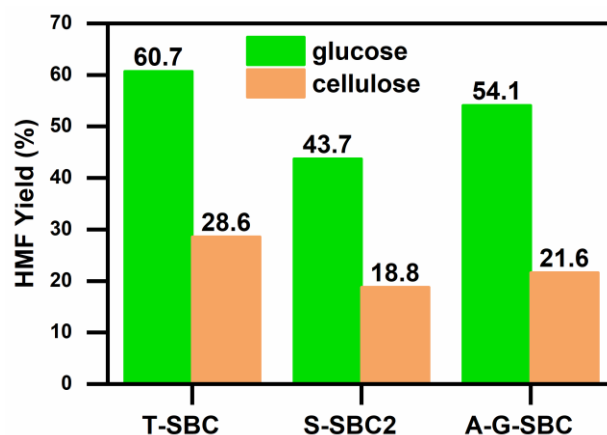

Fig. 8. The catalytic activity of different catalysts for the preparation of HMF from glucose and cellulose (Note: Glucose or cellulose (125 mg), catalyst (100 mg), 10 mL of H$_2$O/THF (1 to 4 ratio v/v), NaCl (0.875 g), and 160 °C for 3 h)

Catalyst reusability

The reusability of a catalyst is an essential parameter for practical applications. To reflect the real cycle performance of a catalyst, the HMF yield was controlled to below 50% by reducing the catalyst loading. Due to the poor catalytic activity of A-SBC, the cyclic performance of A-SBC was not considered here; only the cyclic performance of S-SBC, T-SBC, and A-G-SBC were investigated. In the typical experiment, 100 mg of fructose, 15 mg of T-SBC (or 50 mg of S-SBC or 15 mg of A-G-SBC), and 5 mL of H$_2$O/DMSO (0.5 to 4.5 ratio, v/v) were mixed in the reactor and reacted under the optimum reaction conditions. The recycled catalyst was then filtered, washed, and dried at a temperature of 105 °C for 4 h in the oven. By repeating this operation 5 times, the cyclic performance of the catalyst was determined.

Figure 9 shows the reusability of the catalysts used in this experiment. The catalytic performance of T-SBC and S-SBC remained unchanged after two cycles, which indicated that T-SBC and S-SBC had excellent cycling performance. The yield of HMF when using A-G-SBC considerably decreased during the second use and slightly decreased further during the third time. The catalytic activity remained stable after the third use. This may be because some of the hydrochloric acid molecules were closely adsorbed into the pores and gaps on the surface of the biochar, and a small amount of HCl molecules were desorbed out and entered the solvent system during the reaction. After being used twice, the HCl molecules in the pores were basically stable, and the catalytic activity of A-G-SBC remained basically unchanged.
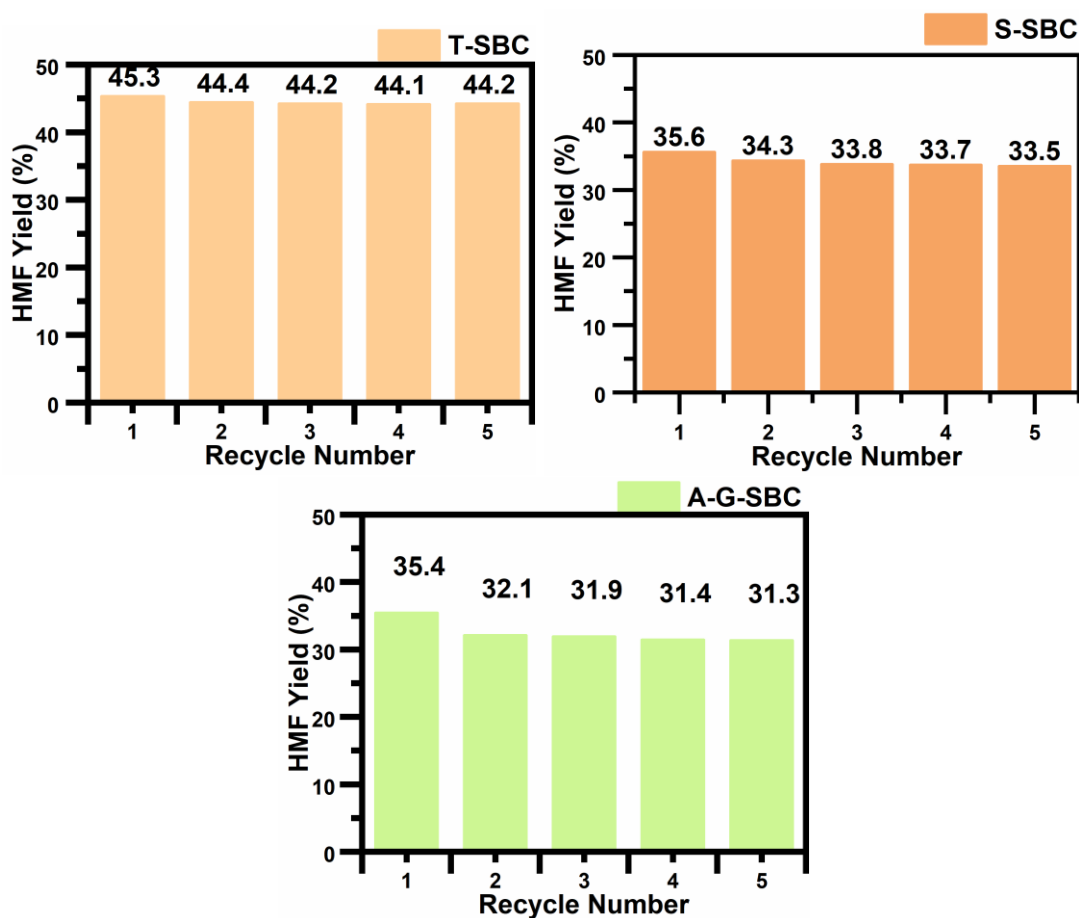
Fig. 9. The catalyst reusability in fructose dehydration to HMF (Note: Yellow: fructose (100 mg), catalyst (15 mg), H_2O/DMSO (0.5 to 4.5 ratio, v/v), 140 °C for 80 min; Orange: fructose (100 mg), catalyst (50 mg), H_2O/DMSO (0.5 to 4.5 ratio, v/v), 160 °C for 60 min; and Green: fructose (100 mg), catalyst (15 mg), H_2O/DMSO ((0.5 to 4.5 ratio, v/v) 130 °C for 40 min)

Proposed dehydration mechanism

The reaction mechanism of the modified biochar with concentrated sulfuric acid is relatively clear; however, the mechanism of p-toluenesulfonic acid and sulfanilic acid is not. Combined with the results of the UV spectrum and catalytic activity, it could be seen that p-toluenesulfonic acid and biochar were involved with a π-π* stacking effect (Fig. 10). If it was assumed that the effect of π-π* stacking played an important role, then p-toluenesulfonic acid could be tightly bound to biochar. In addition, the formation of π-π* stacking may be closely related to the pore size and structure of the biochar surface. P-toluenesulfonic acid had a strong etching effect on the surface of the biochar and could rapidly form many larger mesopores (10 to 50 nm) on the biochar of suitable size. The proper pore and gap structure could facilitate p-toluenesulfonic acid to enter into the biochar and bind to the surface of the biochar. Therefore, T-SBC had good catalytic activity and cycling performance. In addition, since p-toluenesulfonic acid contains a methyl hydrophobic group, there is a further hydrophobic contribution to the hydrophobic biochar, which may be another key role for the tight combination of p-toluenesulfonic acid and biochar (Pratt and Chandler 1977).

The simple calcination method using sulfanilic acid had a weak etching effect on the surface of the biochar and could only form a few micropores, which was not conducive

to the adsorption of sulfanilic acid onto the biochar. At the same time, no π-π* stacking and hydrophobic effects between sulfanilic acid and biochar were present. Therefore, sulfanilic acid could not bind closely with the biochar, resulting in the poor catalytic activity of A-SBC. This conclusion could be verified *via* UV spectral results and nitrogen adsorption analytical test results.
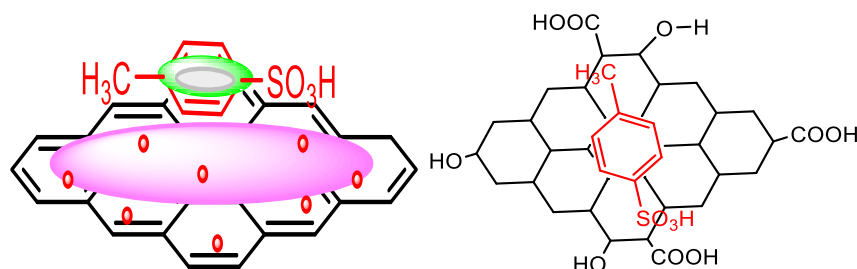

Fig. 10. Schematic diagram of the π-π* stacking in p-toluenesulfonic acid and biochar

The amidation grafting of sulfanilic acid to the biochar surface lifted the restriction of the pore structure. Biochar was oxidized by H_2O_2 to increase the carboxyl group of the biochar. The oxidized biochar was aminated with sulfanilic acid, and then sulfanilic acid was grafted onto the surface of the biochar. The catalyst had excellent catalytic activity and recycling performance, but the preparation process of this method is complicated, with a large amount of water consumption, which has become an obstacle to industrial production.

The H^+ protons were released from the -COOH, -OH, and -SO_3H groups on the surface of the modified biochar. The Bronsted acid attacks the hydroxyl group on the C2 position of the fructose molecule to remove a water molecule, resulting in a carbonium ion. An enol is then formed by losing a proton. Subsequently, HMF is formed after removing two water molecules (as shown in Fig. 11).
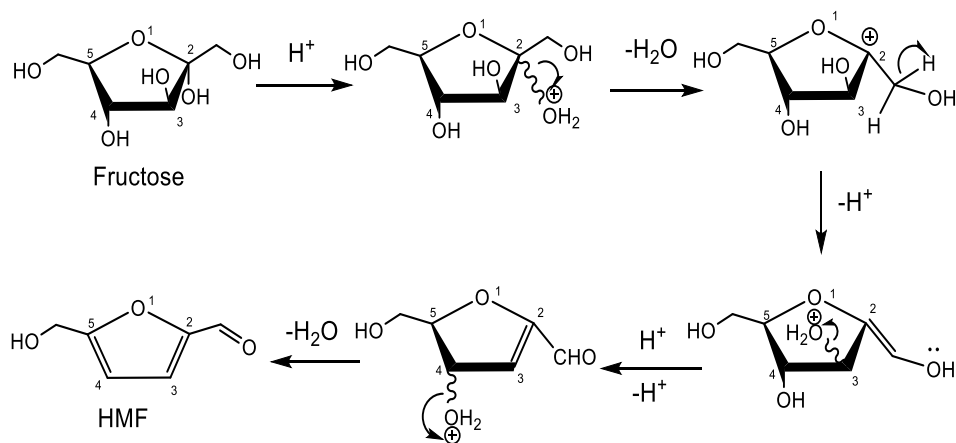

Fig. 11. The mechanism of fructose dehydration to HMF

CONCLUSIONS

1. Carbon-based solid acid was prepared *via* a simple calcination method of concentrated sulfuric acid, p-toluenesulfonic acid, or sulfanilic acid with biochar. The water consumption and the catalytic activity of fructose dehydration to prepare HMF were investigated. The water consumption of 2 g of biochar treated with 6 g of p-toluenesulfonic acid was 750 mL, and the HMF yield was 92.9%. The preparation of A-SBC required the least amount of water for washing but had almost no catalytic activity. The catalytic activity of A-G-SBC prepared *via* the grafting method was greatly improved, and the HMF yield reached 95.2%. However, the water consumption was considerably increased (2500 mL), which became an obstacle to industrial production.

2. The interaction between p-toluenesulfonic acid and biochar was related to the pores and gaps on the surface of the biochar. Suitable mesopores and macropores formed on the surface of the biochar maybe favorable loading of p-toluenesulfonic acid. As such, p-toluenesulfonic acid entered the suitable pores and gaps and bound with the biochar *via* π-π^* stacking or hydrophobic effects. However, there were no suitable pores or gaps on the surface of A-SBC, and no π-π^* stacking and hydrophobic effects between sulfanilic acid and biochar were observed. The amidation grafting of sulfanilic acid to the biochar surface could lift the restriction of the surface pore structure.

3. Carbon-based solid acid was prepared from papermaking sludge and p-toluenesulfonic acid, which has the following advantages: a low cost, simple process, environmentally friendliness, and good catalytic effect, *etc*. It provides an idea for the high value utilization of solid waste and has the potential of industrial production.

ACKNOWLEDGEMENTS

REFERENCES CITED

Bai, Y.-Y., Xiao, L.-P., and Sun, R.-C. (2015). "Microwave-assisted conversion of biomass derived hemicelluloses into xylo-oligosaccharides by novel sulfonated bamboo-based catalysts," *Biomass Bioenergy* 75, 245-253. DOI: 10.1016/j.biombioe.2015.02.023

Boehm, H. P. (1994). "Some aspects of the surface chemistry of carbon blacks and other carbons," *Carbon* 32(5), 759-769. DOI: 10.1016/0008-6223(94)90031-0

Cao, L., Yu , I. K. M., Tsang, D. C. W., Zhang, S., Ok, Y. S., Kwon, E. E., Song, H., and Poon C. S. (2018). "Phosphoric acid-activated wood biochar for catalytic conversion of starch-rich food waste into glucose and 5-hydroxymethylfurfural," *Bioresource Technology* 267, 242-248. DOI: 10.1016/j.biortech.2018.07.048

Cao, L., Yu, I. K. M., Chen, S. S., Tsang, D. C. W., Wang, L., Xiong, X., Zhang, S., Ok, Y. S., Kwon, E. E. Song, H., *et al.* (2018). "Production of 5-hydroxymethylfurfural

from starch-rich food waste catalyzed by sulfonated biochar," *Bioresource Technology* 252, 76-82. DOI: 10.1016/j.biortech.2017.12.098

Cao, Z., Fan, Z., Chen, Y., Li, M., Shen, T., Zhu, C., and Ying, H. (2019). "Efficient preparation of 5-hydroxymethylfurfural from cellulose in a biphasic system over hafnyl phosphates," *Applied Catalysis B: Environment* 244, 170-177. DOI: 10.1016/j.apcatb.2018.11.019

Chen, G., and Fang, B. (2011). "Preparation of solid acid catalyst from glucose–starch mixture for biodiesel production," *Bioresource Technology* 102(3), 2635-2640. DOI: 10.1016/j.biortech.2010.10.099

Corma, A., Iborra, S., and Velty, A. (2007). "Chemical routes for the transformation of biomass into chemicals," *Chemical Reviews* 107(6), 2411-2502. DOI: 10.1021/cr050989d

Gallo, J. M. R., Alamillo, R., and Dumesic, J. A. (2016). "Acid-functionalized mesoporous carbons for the continuous production of 5-hydroxymethylfurfural," *Journal of Molecular Catalysis A: Chemistry* 422, 13-17. DOI: 10.1016/j.molcata.2016.01.005

Gandini, A., and Belgacem, M. N. (2002). "Recent contributions to the preparation of polymers derived from renewable resources," *Journal of Polymers and the Environment* 10, 105-114. DOI: 10.1023/A:1021172130748

Han, B., Zhao, P., He, R., Wu, T., and Wu, Y. (2017). "Catalytic conversion of glucose to 5-hydroxymethyfurfural over B_2O_3 supported solid acids catalysts," *Waste and Biomass Valorization* 9, 2181-2190. DOI: 10.1007/s12649-017-9971-4

Hara, M., Yoshida, T., Takagaki, T., Kondo, J. N., Hayashi, S., and Domen, K. (2004). "A carbon material as a strong protonic acid," *Angewandte Chemie* 43(22), 2955-2958. DOI: 10.1002/anie.200453947

He, R., Huang, X., Zhao, P., Han, B., Wu, T., and Wu, Y. (2018). "The synthesis of 5-hydroxymethylfurfural from glucose in biphasic system by phosphotungstic acidified titanium–zirconium dioxide," *Waste and Biomass Valorization* 9, 657-668. DOI: 10.1007/s12649-017-0024-9

Iris, K., M., and Tsang, D. C. W. (2017). "Conversion of biomass to hydroxymethyl-furfural: A review of catalytic systems and underlying mechanisms," *Bioresource Technology* 238, 716-32. DOI: 10.1016/j.biortech.2017.04.026

Jia, Z., Wang, Y., Shi, W., and Wang, J. (2016). "Diamines cross-linked graphene oxide free-standing membranes for ion dialysis separation," *Journal of Membrane Science* 520, 139-144. DOI: 10.1016/j.memsci.2016.07.042

Kim, R., Qin, W., Wei, G., Wang, G., Wang, L., Zhang, D., Zheng, K., and Liu, N. (2010). "Growth of SiO_2 hierarchical nanostructure on SiC nanowires using thermal decomposition of ethanol and titanium tetrachloride and its FTIR and PL property," *Materials Chemistry and Physics* 119(1-2) 309-314. DOI: 10.1016/j.matchemphys.2009.09.002

Mérida-Morales, S., García-Sancho, C., Oregui-Bengoechea, M., Ginés-Molina, M. J., Cecilia, J. A., Arias, P. L., Moreno-Tost, R., and Maireles-Torres, P. (2021). "Influence of morphology of zirconium-doped mesoporous silicas on 5-hydroxymethylfurfural production from mono-, di- and polysaccharides," *Catalysis Today* 367, 297-309. DOI: 10.1016/j.cattod.2020.02.029

Pang, S., and Wang, B. (2014). "Synthesis of bisphenol A π-π stacking self-assembly imprinted polymer by precipitation polymerization and study on specificity recognition mechanism," *Acta Polymerica Sinica* 2014(1), 49-55. DOI:

10.3724/SP.J.1105.2014.13149

Peng, H. C. (2013). *Theoretical Investigations of Optical and Electronic Property of π-Stacked Molecules*, Master's Thesis, Nanjing University of Posts and Telecommunications, Nanjing, China.

Pratt, L. R., and Chandler, D. (1977). "Theory of the hydrophobic effect," *Journal of Chemical Physics* 67(8), 3683-3704. DOI:10.1063/1.435308.

Priadi, C., Wulandari, D., Rahmatika, I., and Moersidik, S. S. (2014). "Biogas production in the anaerobic digestion of paper sludge," *APCBEE Procedia* 9, 65-69. DOI: 10.1016/j.apcbee.2014.01.012

Shen, Z. (2016). *Study on the Preparation of Sulfonated Carbon Material from Bamboo and its Acidic Catalytic Properties*, Ph.D. Dissertation, Zhejiang University, Hangzhou, China.

Songo, M. M., Moutloali, R., and Ray, S. S. (2019). "Development of TiO_2-carbon composite acid catalyst for dehydration of fructose to 5-hydroxymethylfurfural, catalysts," *Catalysts* 9(2), 1-15. DOI: 10.3390/catal9020126

Sun, X., Wang, J., Chen, J., Zheng, J., Shao, H., and Huang, C. (2018). "Dehydration of fructose to 5-hydroxymethylfurfural over MeSAPOs synthesized from bauxite," *Microporous and Mesoporous Materials* 259, 238-243. DOI: 10.1016/j.micromeso.2017.10.022

Thommes, M., Kaneko, K., Neimark, A. V., Olivier, J. P., Rodriguez-Reinoso, F., Rouquerol, J., and Sing, K. S. W. (2015). *Pure and Applied Chemistry* 87, 1051-1069.

Thoma, C., Konnerth, J., Sailer-Kronlachner, W., Solt, P., Rosenau, T., and Herwijnen H. W. G. (2020). "Current situation of the challenging scale‐Up development of hydroxymethylfurfural production," *ChemSusChem* 13(14), 1-23. DOI: 10.1002/cssc.202000581

Toda, M., Takagaki, A., Okamura, M., Kondo, J. N., Hayasgi, S., Domen, K., and Hara, M. (2005). "Green chemistry: Biodiesel made with sugar catalyst," *Nature* 438, 178. DOI: 10.1038/438178a

Wang, J., Xu, W., Ren, J., Liu, X., Lu, G., and Wang, Y. (2011). "Efficient catalytic conversion of fructose into hydroxymethylfurfural by a novel carbon-based solid acid," *Green Chemistry* 13(10), 2181-2190. DOI: 10.1039/c1gc15306d

Wang, J. J., Tan, Z. C., Zhu, C. C., Miao, G., Kong, L. Z., and Sun, Y. H. (2016). "One-pot catalytic conversion of microalgae (*Chlorococcum* sp.) into 5-hydroxymethyl-furfural over the commercial H-ZSM-5 zeolite," *Green Chemistry* 18(2) 452-460. DOI: 10.1039/c5gc01850a

Wang, C., Yang, G., Zhang, X., Shao, L., Lyu, L., Mao, J., Liu, S., and Xu, F. (2019). "A kinetic study on the hydrolysis of corncob residues to levulinic acid in the $FeCl_3$-NaCl system," *Cellulose* 26, 8313-8323. DOI: 10.1007/s10570-019-02711-7

Wrigstedt, P., Keskiväli, J., and Rero, T. (2016). "Microwave-enhanced aqueous biphasic dehydration of carbohydrates to 5-hydroxymethylfurfural," *RSC Advances* 6(23), 18973-18979. DOI: 10.1039/c5ra25564c

Xu, J., Xu, X., Liu, Y., Li, H., and Liu, H. (2015). "Effect of microbiological inoculants DN-1 on lignocellulose degradation during co-composting of cattle manure with rice straw monitored by FTIR and SEM," *Environmental Progress & Sustainable Energy* 35(2), 345-351. DOI: 10.1002/ep.12222

Zhang, C., Cheng, Z., Fu, Z., Liu, Y., Yi, X., Zheng, A., Kirk, S. R., and Yin, D. (2017). "Effective transformation of cellulose to 5-hydroxymethylfurfural catalyzed by

fluorine anion-containing ionic liquid modified biochar sulfonic acids in water," *Cellulose* 24, 95-106. DOI: 10.1007/s10570-016-1118-4

Zhang, W., Zhang, X., Lei, F., and Jiang, J. (2020). "Co-production bioethanol and xylooligosaccharides from sugarcane bagasse *via* autohydrolysis pretreatment," *Renewable Energy* 162, 2297-2305. DOI: 10.1016/j.renene.2020.10.034

Zhao, J., Zhou, C., He, C., Dai, Y., Jia, X., and Yang, Y. (2016). "Efficient dehydration of fructose to 5-hydroxymethylfurfural over sulfonated carbon sphere solid acid catalysts," *Catalysis Today* 264, 123-130. DOI: 10.1016/j.cattod.2015.07.005

Zhao, F. G., Hu, C. M., Kong, Y. T., Pan, B., and Li, W. S. (2018). "Sulfanilic acid pending on graphene scaffold: Novel, efficient synthesis and much enhanced polymer solar cell efficiency and stability using it as hole extraction layer," *ACS Applied Materials & Interfaces* 10(29). DOI:10.1021/acsami.8b06562